



# Warm and dense gas and dust in Carina

Carsten Kramer

KOSMA

I. Physikalisches Institut  
Universität zu Köln, Germany

# NANTEN2 Submillimeter Observatory



ALMA site at 4685m altitude

Consortium of universities:  
Nagoya (Prof. Y.Fukui),  
Osaka, Köln, Bonn, Seoul,  
Sydney, Zürich, Santiago

Science with NANTEN2:

Large-scale distribution, dynamics,  
and chemistry of the ISM in the  
Milky Way and in external galaxies

230 GHz – 880 GHz  
low- and mid-J CO,  $^{13}\text{CO}$  lines  
fine structure lines of atomic carbon

First results from 2006/7:

talk by T.Onishi (LMC)

poster P14 by J.Pineda (N159W/LMC)

poster P4 by M.Hitschfeld (Circinus & NGC4945)

poster P17 by R.Simon (Rosette)

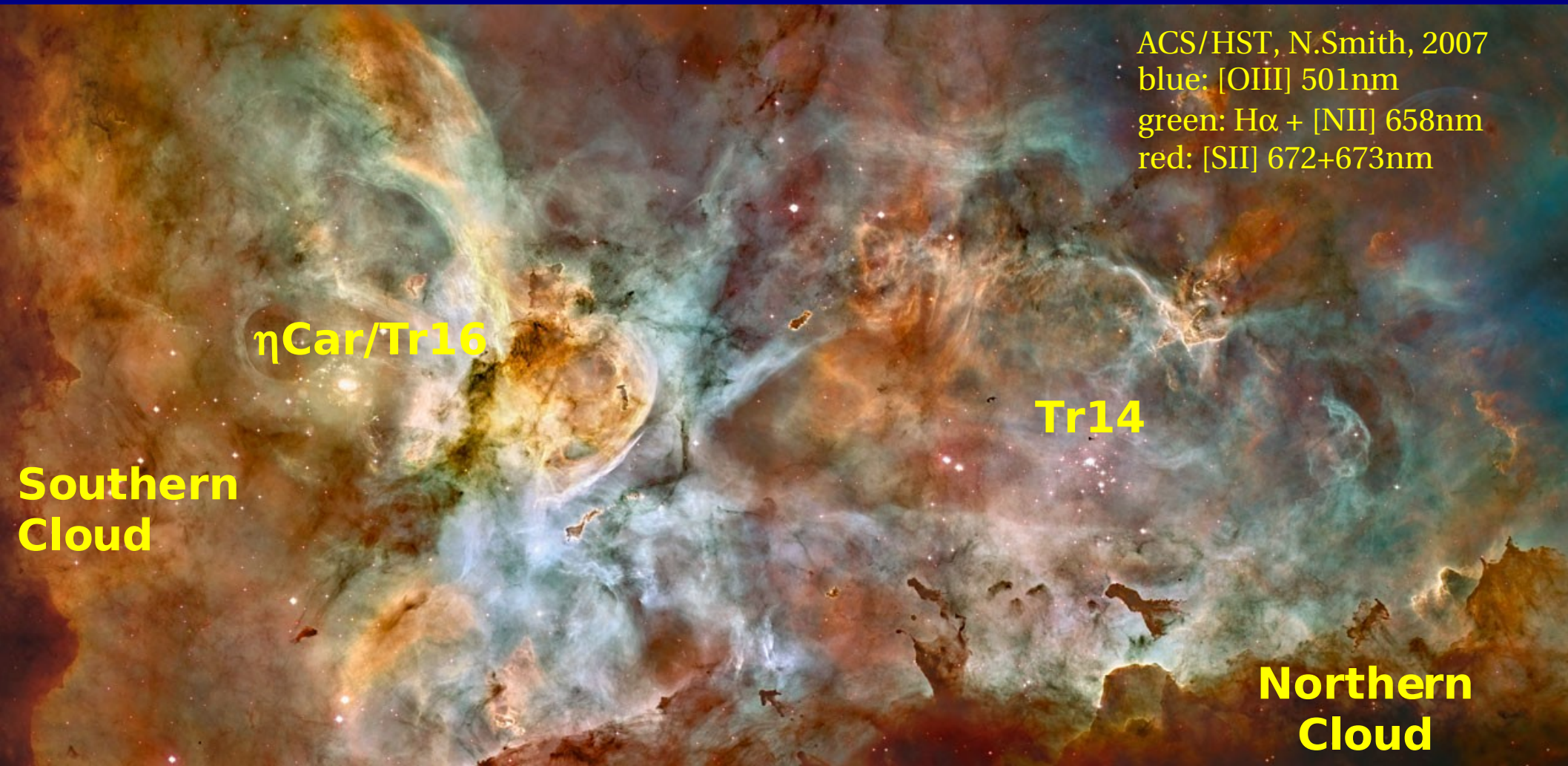
# Warm and dense gas and dust in Carina



ACS/HST, N.Smith, 2007  
blue: [OIII] 501nm  
green: H $\alpha$  + [NII] 658nm  
red: [SII] 672+673nm

**Kramer, C. and the NANTEN2 team,  
accepted by A&A**

# Warm and dense gas and dust in Carina



ACS/HST, N.Smith, 2007  
blue: [OIII] 501nm  
green: H $\alpha$  + [NII] 658nm  
red: [SII] 672+673nm

$\eta$ Car/Tr16

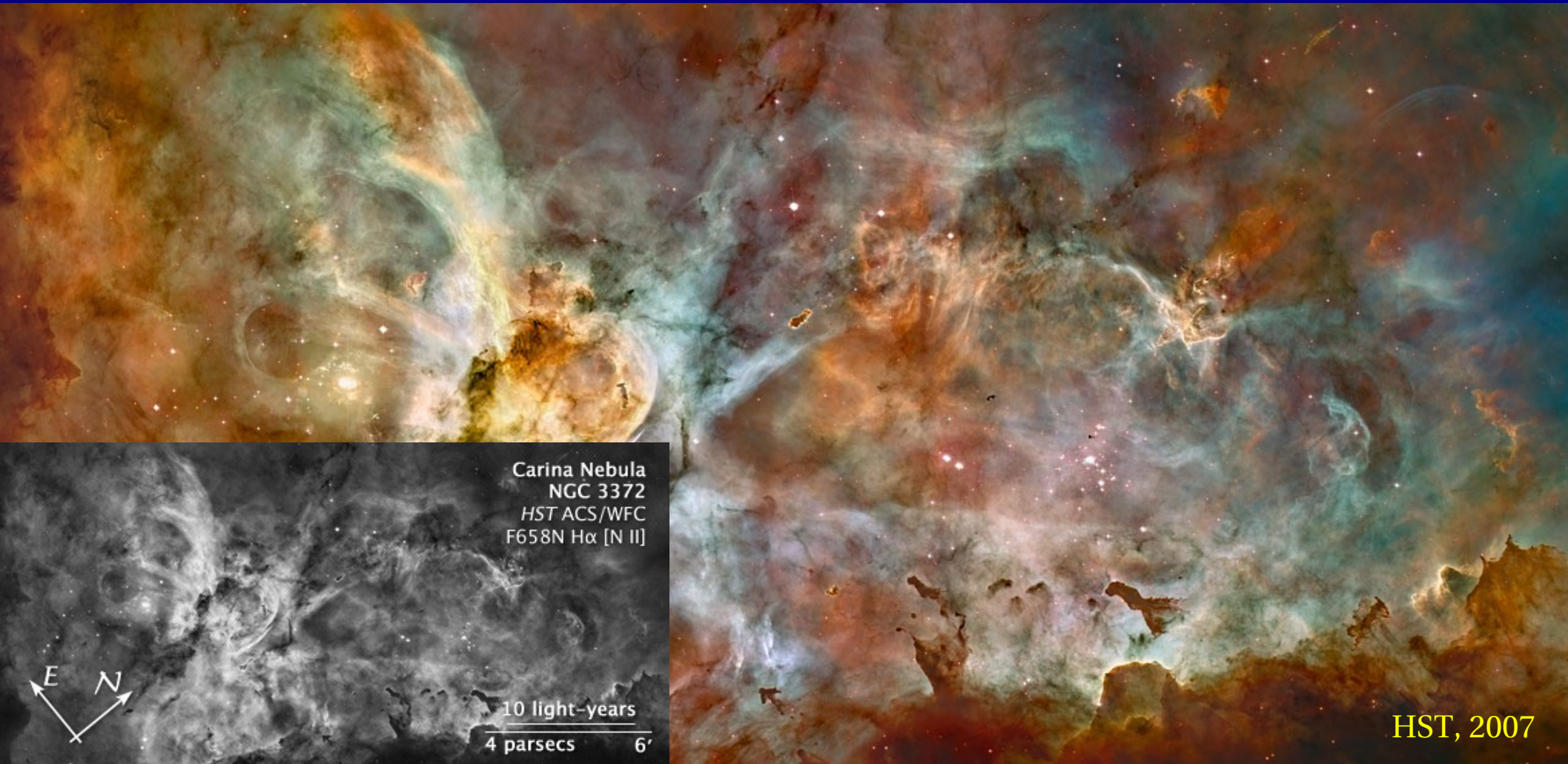
Tr14

Southern  
Cloud

Northern  
Cloud

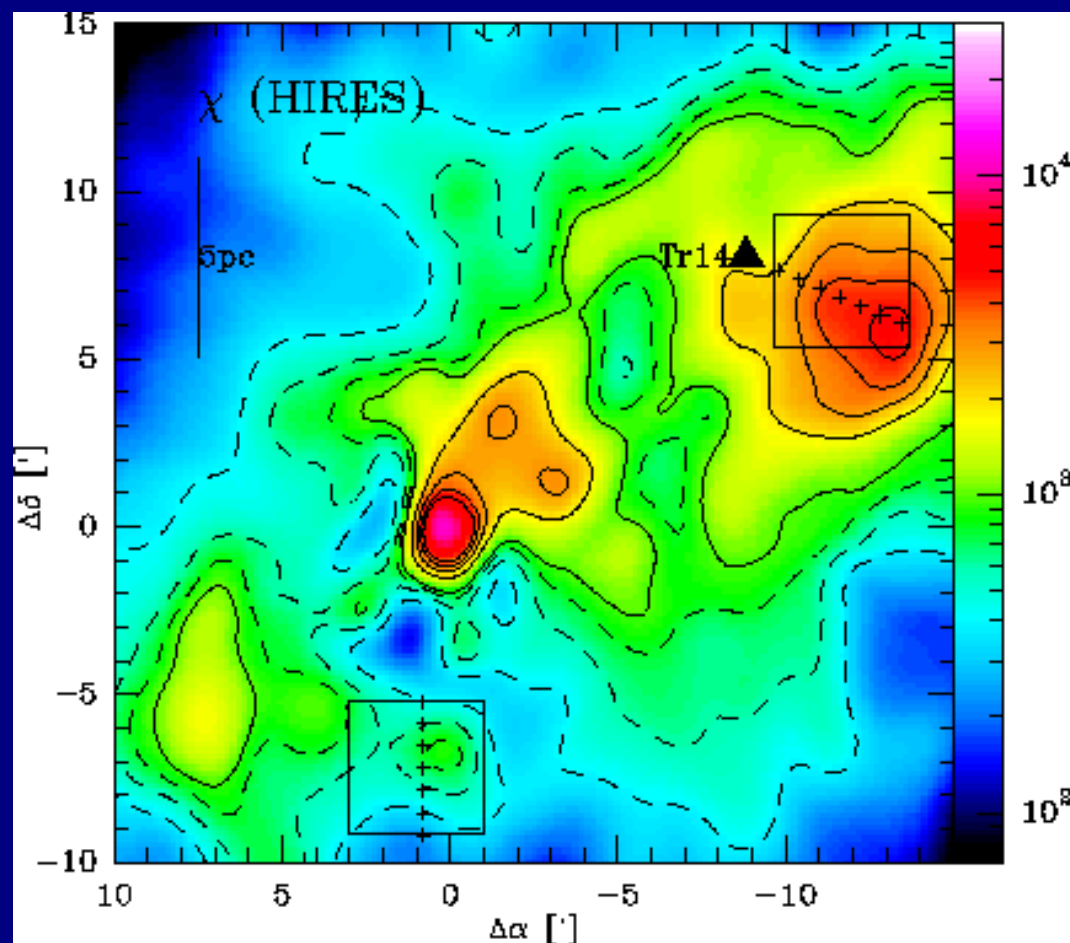
**Kramer, C. and the NANTEN2 team,  
accepted by A&A**

# Warm and dense gas and dust in Carina



**Kramer, C. and the NANTEN2 team,  
accepted by A&A**

# Estimating the FUV field in Carina



FUV-fluxes estimated from HIRES data.  
Northern and Southern 4'x4' NANTEN2  
fields with cuts.

HIRES/IRAS data at 60 $\mu$ m, 100 $\mu$ m  
FIR continuum (40-120 $\mu$ m):

$$\left( \frac{I_{\text{FIR}}}{\text{ergs s}^{-1} \text{ cm}^{-2} \text{ sr}^{-1}} \right) = 3.25 \times 10^{-11} \left[ \frac{f_{\nu}(60 \mu\text{m})}{\text{Jy sr}^{-1}} \right] + 1.26 \times 10^{-11} \left[ \frac{f_{\nu}(100 \mu\text{m})}{\text{Jy sr}^{-1}} \right].$$

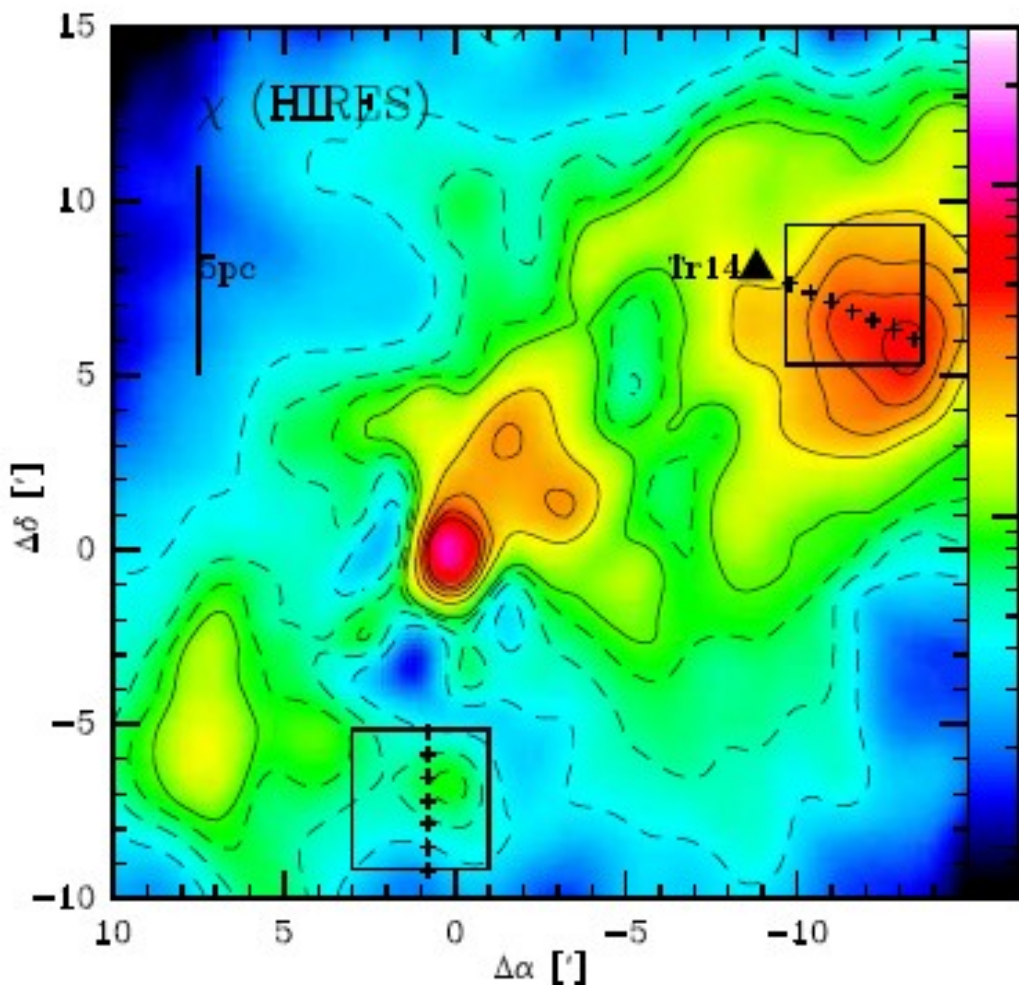
(Nakagawa et al. 1998)

$$\chi/\chi_0 = 4\pi I_{\text{FIR}} / (\text{erg s}^{-1} \text{ cm}^{-2} \text{ sr}^{-1})$$

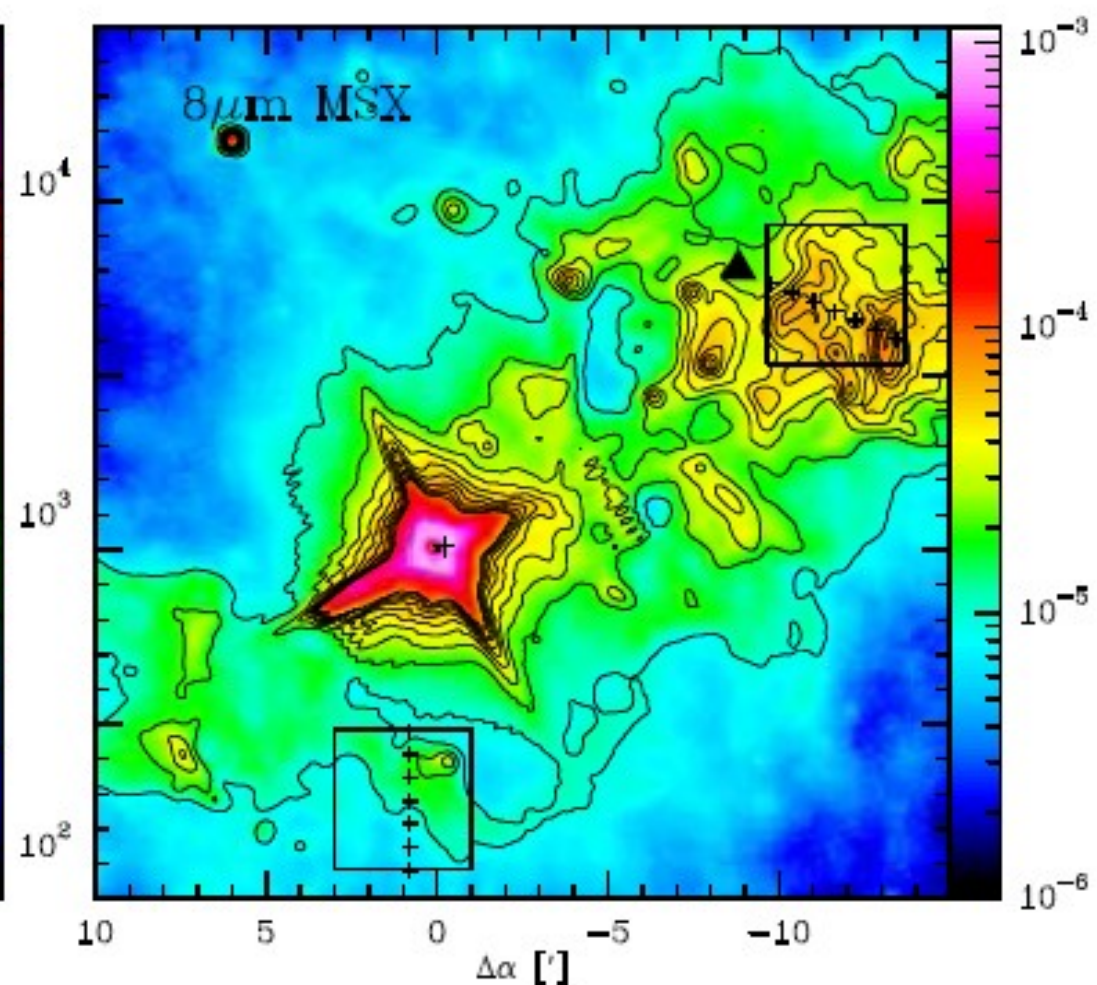
FUV-flux in Draine units  
(6eV < hv < 13.6eV):

400, 600, 800  $\chi_0$  (dashed contours)  
(1, 2, 3, 4, 5)  $10^3 \chi_0$  (drawn contours)

# Dust and PAHs in Carina

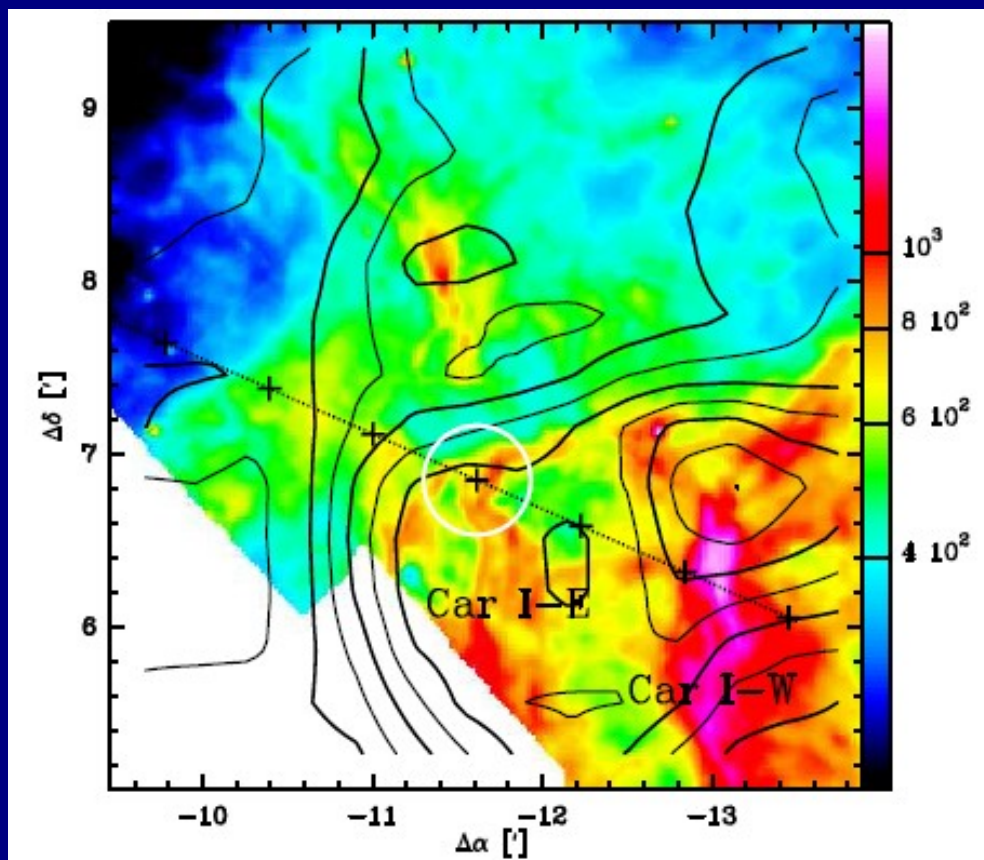


Colors: FUV-field derived from HIRES

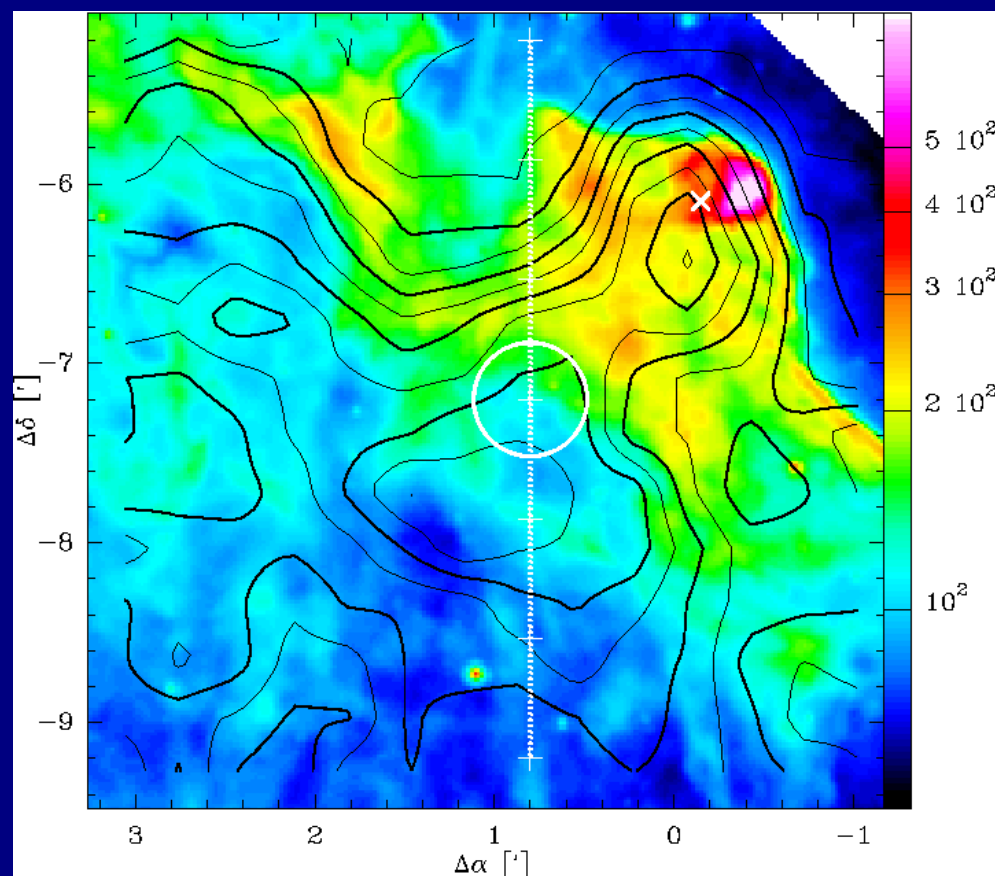


Colors: 8  $\mu\text{m}$  MSX

# NANTEN2-fields: CO 4-3 and 8 $\mu$ m IRAC

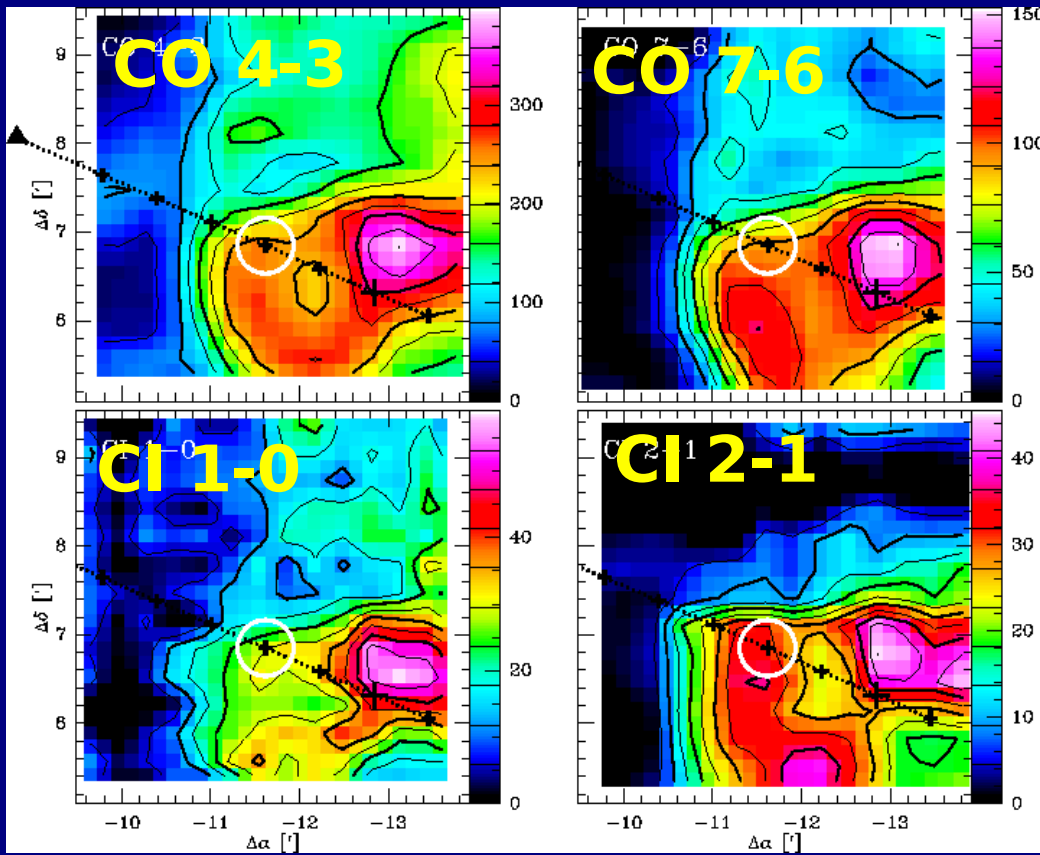


Northern field:  
Contours: CO 4-3 integrated intensity  
Colors: 8 $\mu$ m IRAC/Spitzer.  
38" resolution (0.43pc)

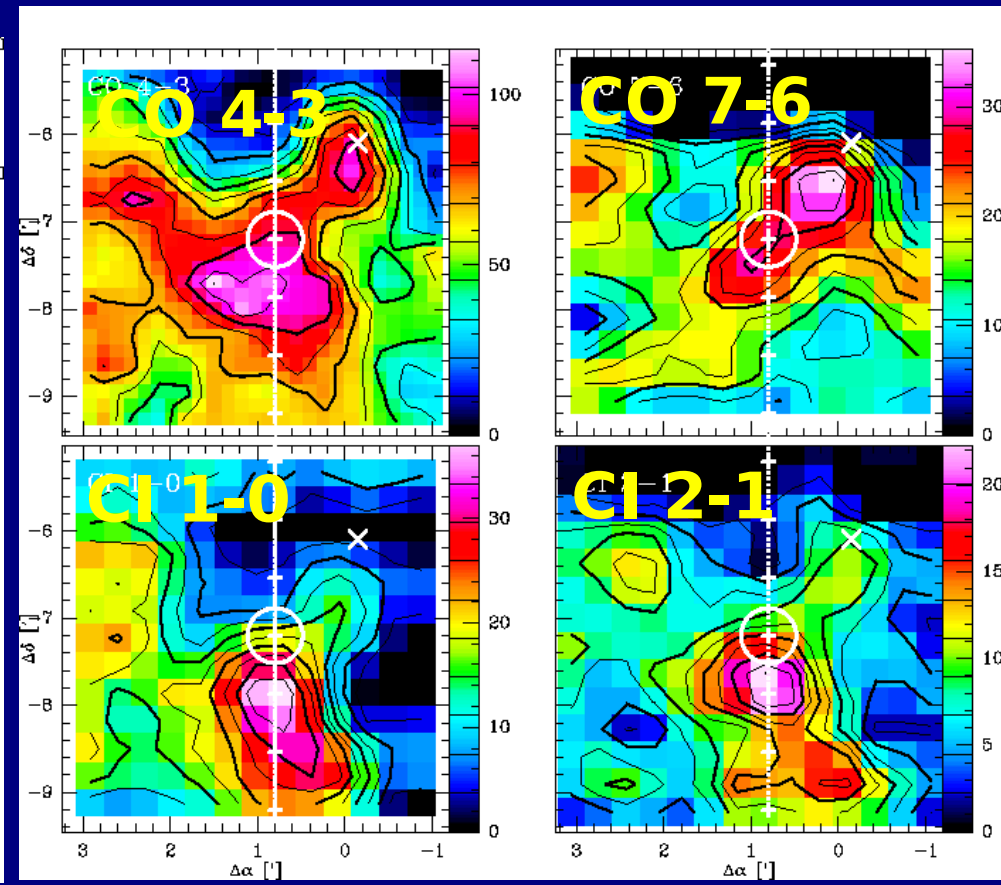


Southern field

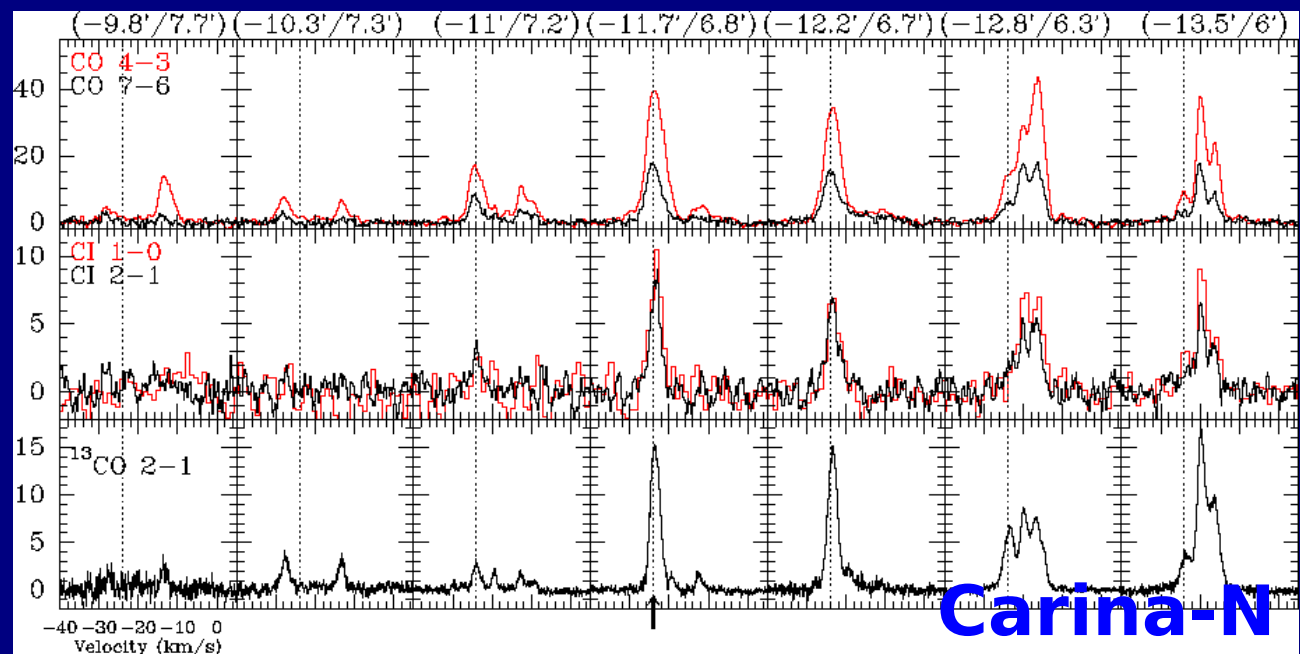
# Carina-N:



# Carina-S:



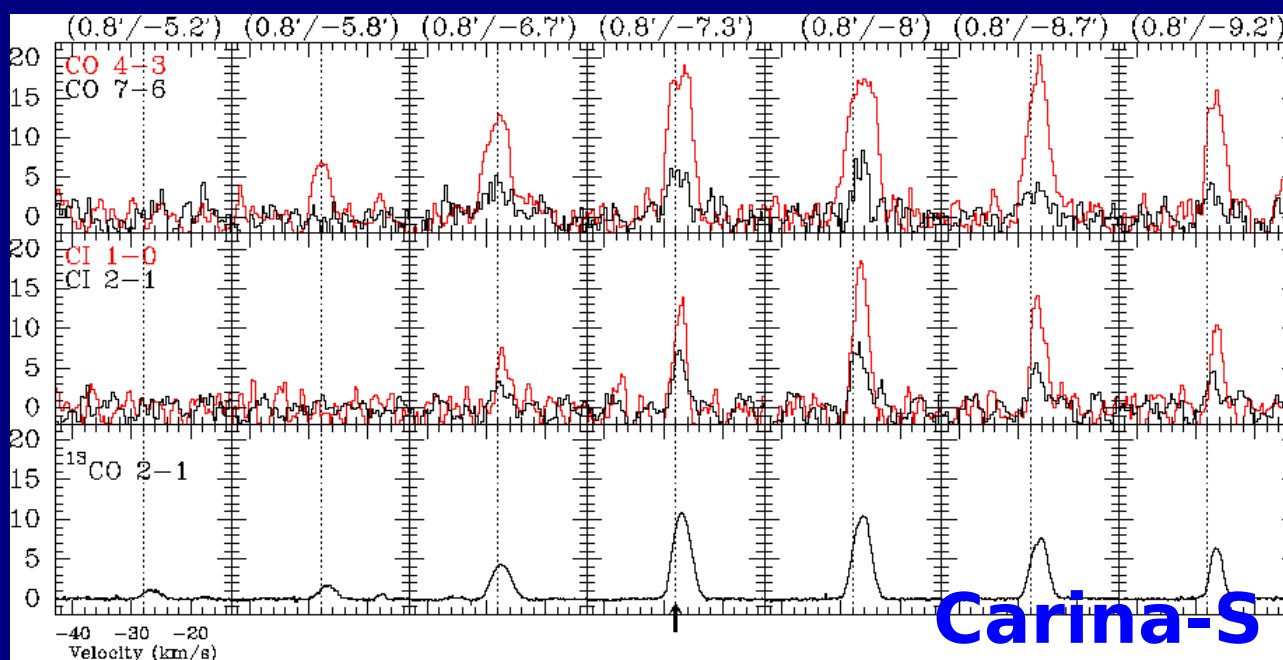
# Cuts through the 2 interfaces:



CO 4-3, 7-6 (NANTEN2)

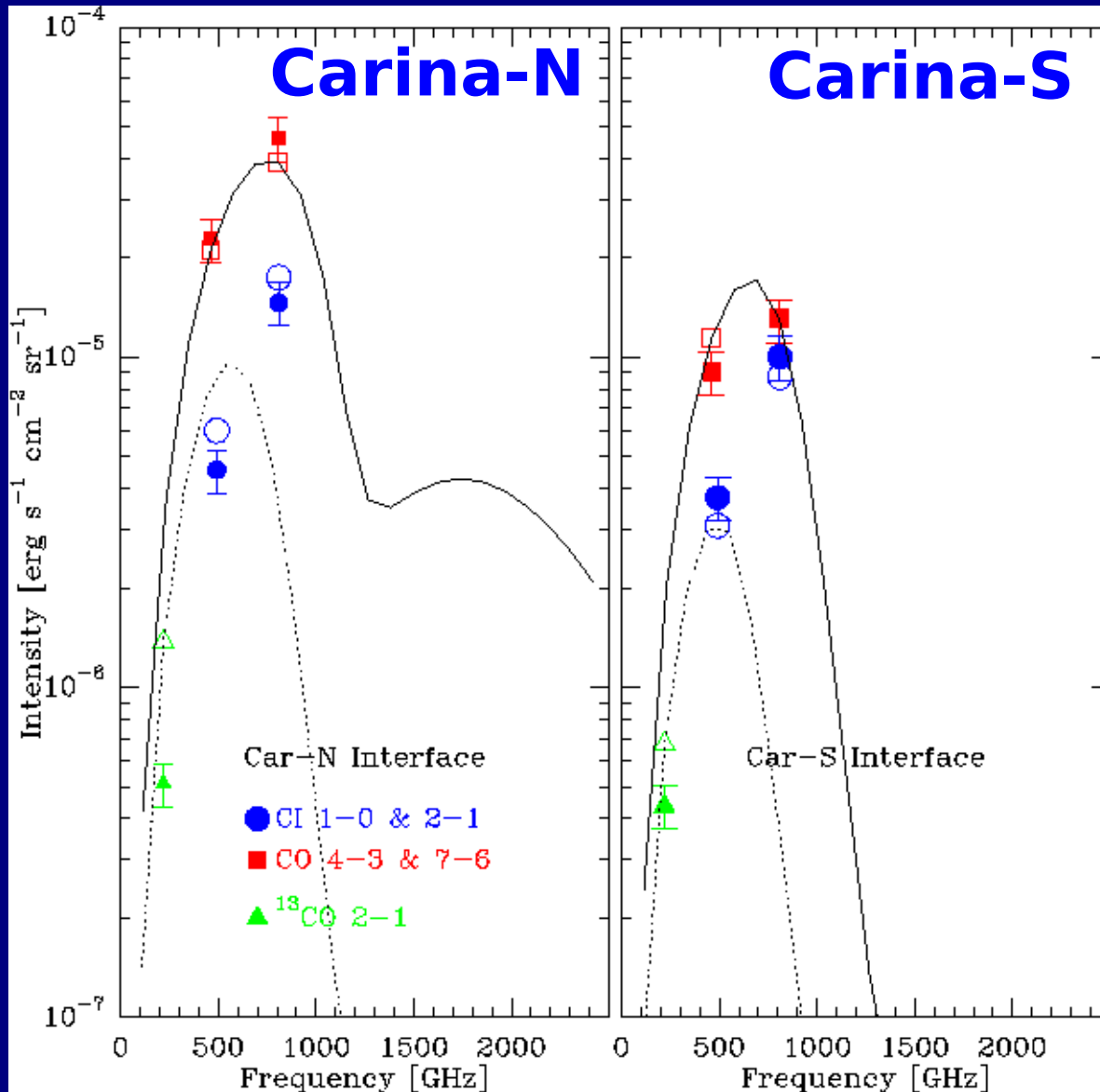
[CI] 1-0, 2-1 (NANTEN2)

<sup>13</sup>CO 2-1 (SEST;  
Brooks et al. 2003)



FWHMs from Gaussian fits  
at the 2 interface positions:  
North: 2.9 - 5.4 km/s  
South: 2.1 - 4.3 km/s

# Two interface positions:



Observed and modelled cooling intensities of  
[CI] 1-0, 2-1, CO 4-3, 7-6,  $^{13}\text{CO}$  2-1

# PDR modelling:

Modelling using the KOSMA- $\tau$  PDR model of spherically symmetric clumps, and the approach developed by Markus Cubick:

1. Calculate clump average line intensity as function of FUV field, mass, density (with clump internal density profile)
2. Assume an ensemble of clumps within each beam:
  - power-law mass distribution ( $dN/dM \sim M^{-\alpha}$ ,  $\alpha = 1.7$ , e.g. Simon et al. 2001)
  - power-law mass size relation ( $M \sim R^\gamma$ ,  $\gamma = 2.3$ , e.g. Heithausen et al. 1998)Resulting clump density distribution:  $n \sim M^{1-3/\gamma}$

Create lookup-table of volume emissivity of [C I], CO lines, as function of

- FUV field
- mass density
- average clump ensemble density

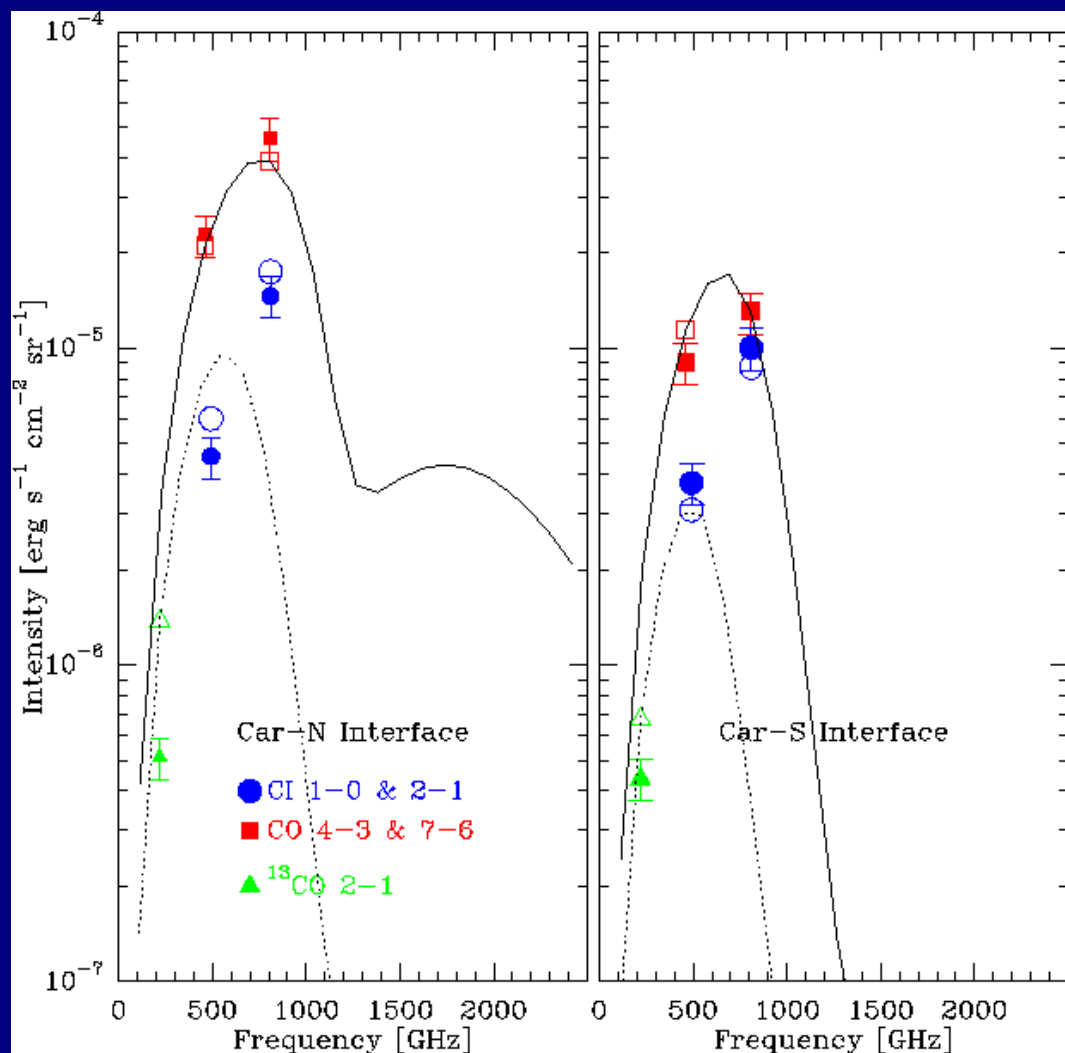
3. Specify 3-dimensional distribution of source structure.

Simplest approach chosen here:

assume that emitting regions is characterized by one FUV field,  $M_{\text{tot}}$ ,  $\langle n \rangle$

- (4. Line-of-sight integration to get 2-dimensional intensity distribution.)

# PDR modelling results:



FUV estimated from HIRES data

Free parameter to fit line ratios:  
average ensemble density

$$\langle n \rangle_{\text{ens}} = 2 \cdot 10^5 \text{ cm}^{-3}$$

Free parameter to fit absolute intensities:

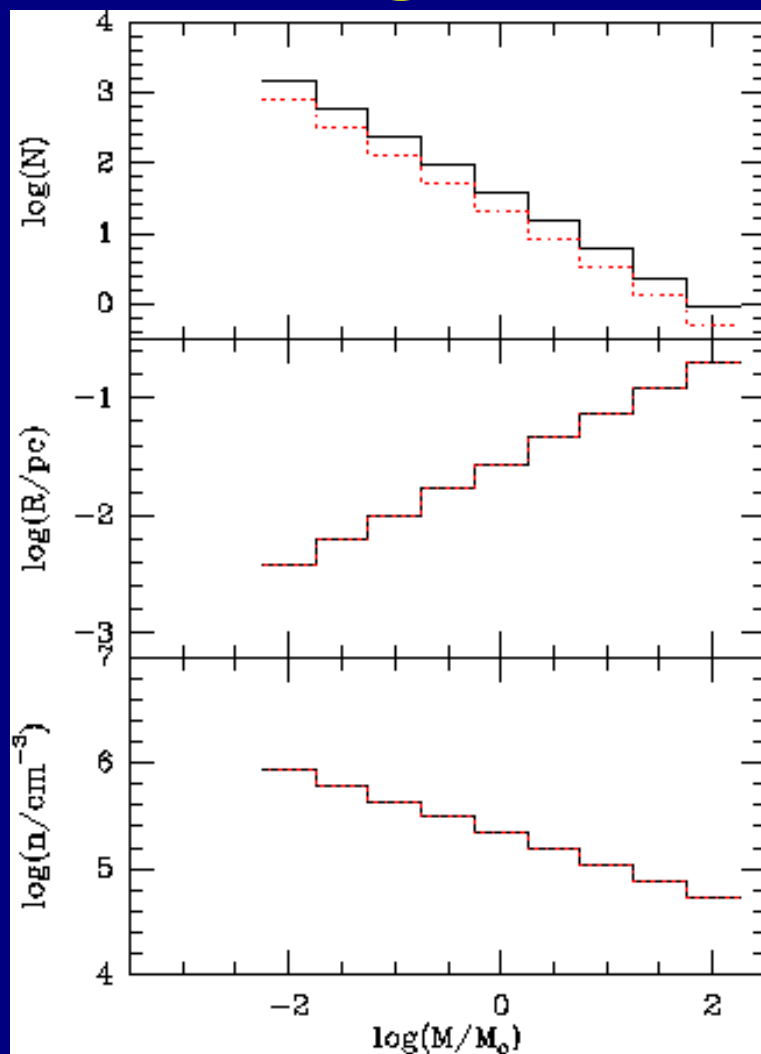
total ensemble mass

$$M_{\text{tot}} = 220 \text{ and } 400 M_{\text{sun}}$$

Modelled intensities of  
[CI], CO agree to within 20%,  
<sup>13</sup>CO 2-1 agrees within a factor 2.

$\Delta\alpha/\Delta\delta$ (',')	$\chi$	$\langle n \rangle_{\text{ens}}$ $\text{cm}^{-3}$	$M_{\text{cl}}^{\text{min}}$ $M_{\odot}$	$M_{\text{cl}}^{\text{max}}$ $M_{\odot}$	$M_{\text{tot}}$ $M_{\odot}$	$n_{0,\text{min}}$ $\text{cm}^{-3}$	$n_{0,\text{max}}$ $\text{cm}^{-3}$	$R_{\text{min}}$ pc	$R_{\text{max}}$ pc	$\phi_A$
(1)	(2)	(3)	(4)	(5)	(6)	(7)	(8)	(9)	(10)	(11)
-11.7/6.8	$10^{3.5}$	$2 \cdot 10^5$	$10^{-2}$	$10^2$	400	$5.3 \cdot 10^4$	$8.8 \cdot 10^5$	$3.7 \cdot 10^{-3}$	$2.1 \cdot 10^{-1}$	3.9
+0.8/-7.2	$10^{2.5}$	$2 \cdot 10^5$	$10^{-2}$	$10^2$	220	$5.3 \cdot 10^4$	$8.8 \cdot 10^5$	$3.7 \cdot 10^{-3}$	0.2	2.1

# PDR modelling results:



Clump power-law distributions:

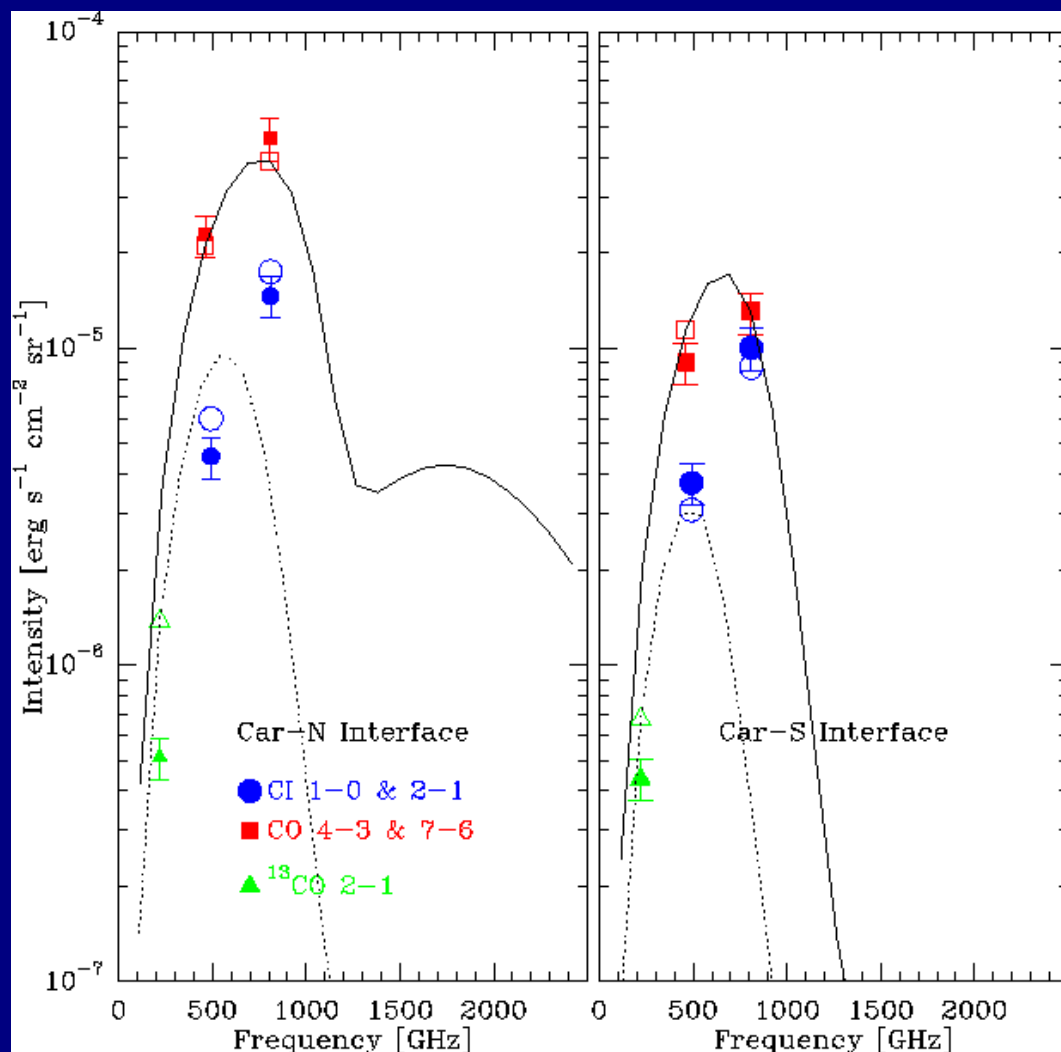
Number of clumps vs. masses

Clump radii vs. masses

Clump densities vs. masses

$\Delta\alpha/\Delta\delta$ (',')	$\chi$	$\langle n \rangle_{\text{ens}}$ $\text{cm}^{-3}$	$M_{\text{cl}}^{\text{min}}$ $M_{\odot}$	$M_{\text{cl}}^{\text{max}}$ $M_{\odot}$	$M_{\text{tot}}$ $M_{\odot}$	$n_{0,\text{min}}$ $\text{cm}^{-3}$	$n_{0,\text{max}}$ $\text{cm}^{-3}$	$R_{\text{min}}$ pc	$R_{\text{max}}$ pc	$\phi_A$
(1)	(2)	(3)	(4)	(5)	(6)	(7)	(8)	(9)	(10)	(11)
-11.7/6.8	$10^{3.5}$	$2 \cdot 10^5$	$10^{-2}$	$10^2$	400	$5.3 \cdot 10^4$	$8.8 \cdot 10^5$	$3.7 \cdot 10^{-3}$	$2.1 \cdot 10^{-1}$	3.9
+0.8/-7.2	$10^{2.5}$	$2 \cdot 10^5$	$10^{-2}$	$10^2$	220	$5.3 \cdot 10^4$	$8.8 \cdot 10^5$	$3.7 \cdot 10^{-3}$	0.2	2.1

# PDR modelling results:



Robustness against mass limits:

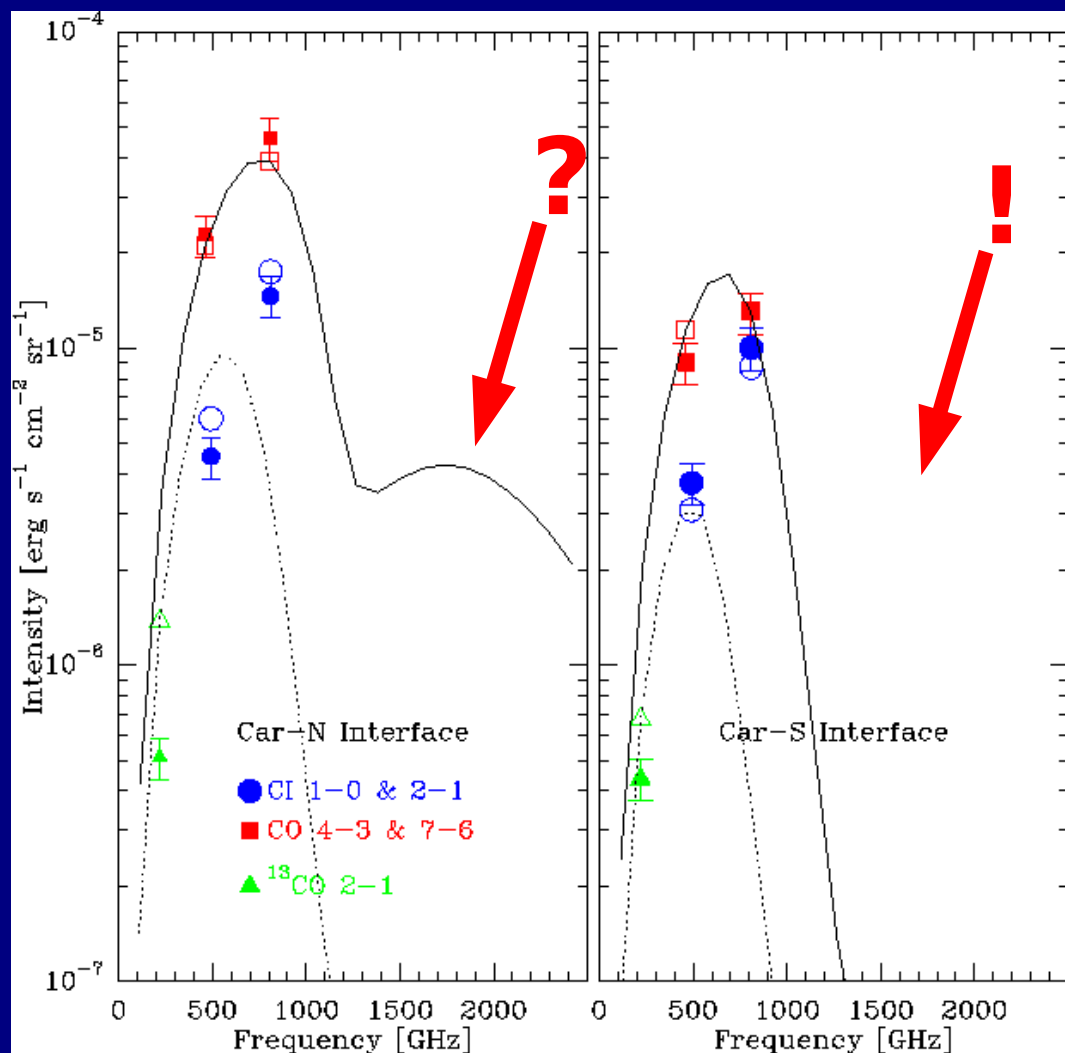
Modelled intensities vary by less than a factor 2

for  $10^{-1} < M_{\min}/M_{\text{sun}} < 10^{-3}$

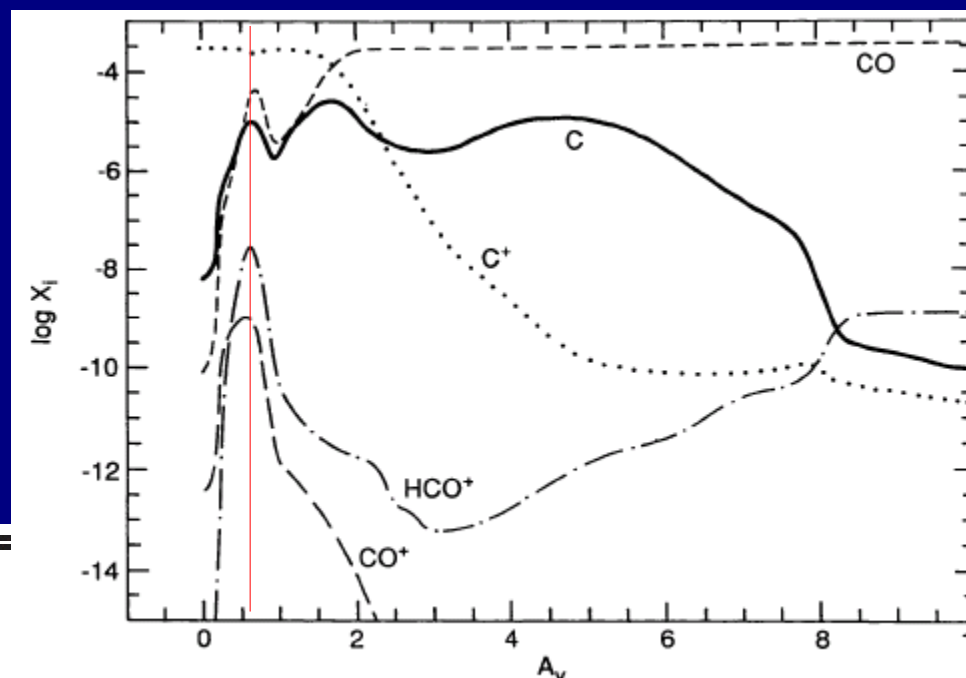
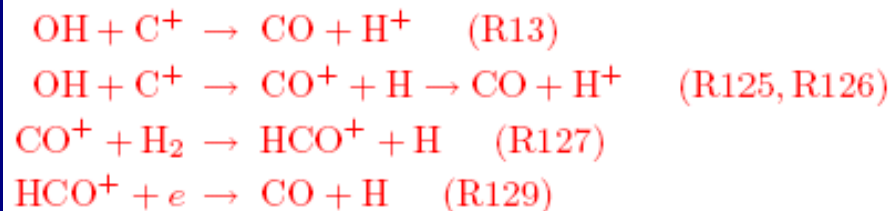
and for  $10^1 < M_{\max}/M_{\text{sun}} < 10^3$ .

$\Delta\alpha/\Delta\delta$ (',')	$\chi$	$\langle n \rangle_{\text{ens}}$ $\text{cm}^{-3}$	$M_{\text{cl}}^{\text{min}}$ $M_{\odot}$	$M_{\text{cl}}^{\text{max}}$ $M_{\odot}$	$M_{\text{tot}}$ $M_{\odot}$	$n_{0,\text{min}}$ $\text{cm}^{-3}$	$n_{0,\text{max}}$ $\text{cm}^{-3}$	$R_{\text{min}}$ pc	$R_{\text{max}}$ pc	$\phi_A$
(1)	(2)	(3)	(4)	(5)	(6)	(7)	(8)	(9)	(10)	(11)
-11.7/6.8	$10^{3.5}$	$2 \cdot 10^5$	$10^{-2}$	$10^2$	400	$5.3 \cdot 10^4$	$8.8 \cdot 10^5$	$3.7 \cdot 10^{-3}$	$2.1 \cdot 10^{-1}$	3.9
+0.8/-7.2	$10^{2.5}$	$2 \cdot 10^5$	$10^{-2}$	$10^2$	220	$5.3 \cdot 10^4$	$8.8 \cdot 10^5$	$3.7 \cdot 10^{-3}$	0.2	2.1

# PDR modelling results: Hot CO



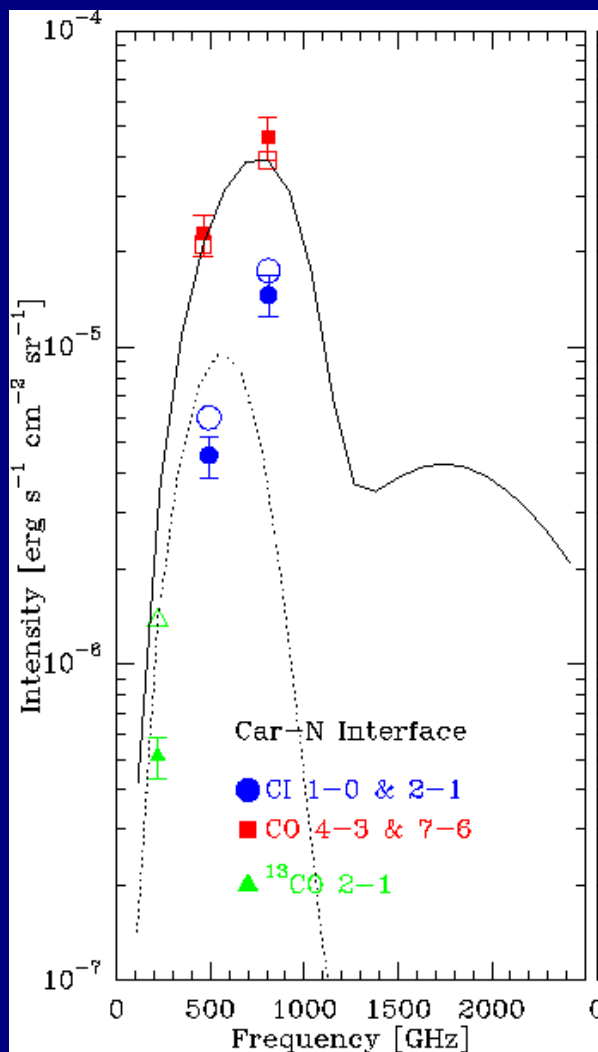
The CO abundance is increased in the hot HI/H<sub>2</sub> surface layer, near the OH density peak (Sternberg & Dalgarno 1995):



$\Delta\alpha/\Delta\delta$ (',')	$\chi$ (2)	$\langle n \rangle_{\text{ens}}$ $\text{cm}^{-3}$ (3)	$M_{\text{cl}}^{\text{min}}$ $M_{\odot}$ (4)	$M_{\text{cl}}^{\text{max}}$ $M_{\odot}$ (5)	$M_{\text{tot}}$ $M_{\odot}$ (6)
-11.7/6.8	$10^{3.5}$	$2 \cdot 10^5$	$10^{-2}$	$10^2$	400
+0.8/-7.2	$10^{2.5}$	$2 \cdot 10^5$	$10^{-2}$	$10^2$	220

FIG. 11a  
 $5.3 \cdot 10^4$     $8.8 \cdot 10^5$     $3.7 \cdot 10^{-3}$    0.2   2.1

# PDR modelling:



Remarks:

- clumps do not shadow (Area filling factors < 4)
- clumps with  $M < 10^{-2} M_{\text{sun}}$  do exist

- clumps have constant  $\Delta v = 1.7 \text{ kms}^{-1}$

Small clumps are not virialized:

$$M_{\text{vir}} / M_{\text{min}} = 400 \text{ for } M_{\text{min}} = 0.01 M_{\text{sun}}$$

$$t_{\text{evap}} = 5000 \text{ yrs}$$

$$P_{\text{ext}} = 10^8 \text{ Kcm}^{-3}.$$

- The interclump medium is ignored:

No CI, CO emission from the interclump medium.

No pre-shielding by  $\text{H}_2$  (but see Bensch et al. 2003).

$\Delta\alpha/\Delta\delta$ (',')	$\chi$	$\langle n \rangle_{\text{ens}}$ $\text{cm}^{-3}$	$M_{\text{cl}}^{\text{min}}$ $M_{\odot}$	$M_{\text{cl}}^{\text{max}}$ $M_{\odot}$	$M_{\text{tot}}$ $M_{\odot}$	$n_{0,\text{min}}$ $\text{cm}^{-3}$	$n_{0,\text{max}}$ $\text{cm}^{-3}$	$R_{\text{min}}$ pc	$R_{\text{max}}$ pc	$\phi_A$ (11)
(1)	(2)	(3)	(4)	(5)	(6)	(7)	(8)	(9)	(10)	(11)
-11.7/6.8	$10^{3.5}$	$2 \cdot 10^5$	$10^{-2}$	$10^2$	400	$5.3 \cdot 10^4$	$8.8 \cdot 10^5$	$3.7 \cdot 10^{-3}$	$2.1 \cdot 10^{-1}$	3.9
+0.8/-7.2	$10^{2.5}$	$2 \cdot 10^5$	$10^{-2}$	$10^2$	220	$5.3 \cdot 10^4$	$8.8 \cdot 10^5$	$3.7 \cdot 10^{-3}$	0.2	2.1



## Summary/Outlook

- NANTEN2 observations of two 4'x4' fields in Carina in  $^{12}\text{CO}$  4-3 & 7-6, [CI] 1-0, 2-1
- combined with SEST  $^{13}\text{CO}$  2-1
- FUV field estimate from HIRES/IRAS (400 – 5000  $\chi_0$ )
- Correlation with 8 $\mu\text{m}$  IRAC/Spitzer maps
- Clumpy PDR models (KOSMA- $\tau$ ) consistent with observed CO, [CI] intensities within 20%, i.e. within the calibration accuracy.
- Ongoing and future projects to study PDR chemistry with NANTEN2, APEX, Mopra, Herschel